

Measurement of Small-Scale Fading Distributions in a Realistic 2.4 GHz Channel

*Alexander H. Henderson,
Furman University, Greenville, SC,
29613*

*Prof. Gregory D. Durgin and
Christopher J. Durkin, Georgia
Institute of Technology, Atlanta, GA
30332*

Introduction

Characterization of wireless signal fading is of growing interest due to the proliferation of cell phones, wireless monitoring equipment, and other wireless devices. While large-scale fading typically describes relative reception over distances many times the wavelength(s) being considered, small-scale fading leads to the most unpredictable dips in transmission strength or even complete loss of signal (a “null”) and consequent termination of the connection [1, p.34]. Consequently, information on small-scale fading and how to correct for it proves useful to radio designers.

Small-scale fading refers to the varying strength of wireless signals within a local area due to the constructive and destructive interference of multipath waves resulting from reflection and diffraction off of nearby scattering surfaces [1, p.34]. It is typically assumed that in such a situation, Rayleigh statistics will be the worst possible distribution in terms of points where the signal strength drops below a certain pre-determined threshold [1, pp. 7-8], while a Ricean curve is used to describe a case of one strong line-of-sight element with all other contributions being weaker, which is a good approximation for certain real situations [1, pp. 127-128]. Work by Frolik indicates that certain situations experience “Hyper-Rayleigh” fading, though this occurs only in specific, highly dispersive cases [3].

Rayleigh statistics assumes that there are no specular wave components and a diffuse, nonspecular component. A specular component is an individual electromagnetic wave, here assumed to be of significant strength by itself, while a diffuse component is one which is composed of a number of waves whose individual strengths are small in comparison to the component’s total strength. The Ricean model, conversely, assumes that there is a single specular component, which is typically a line-of-sight component, in addition to the diffuse

component. Mathematically, the probability density function (pdf) for a Rayleigh distribution is $\frac{r^2}{\sigma^2} \exp\left(\frac{-r^2}{2\sigma^2}\right)$, where r is the magnitude of the received voltage and σ^2 is the variance in the data. A Ricean pdf is $\frac{r^2}{\sigma^2} \exp\left(\frac{-r^2 - V_1^2}{2\sigma^2}\right) I_0\left(\frac{rV_1}{\sigma^2}\right)$, where r and σ^2 are as above, V_1 is the magnitude of the voltage of the specular component, and $I_0(.)$ is a zeroth-order modified Bessel function.

There have been many measurement campaigns to characterize the wireless channel for large-scale fading. Propagation characteristics inside buildings used for various industrial, laboratory, and office purposes have been conducted at various frequencies and under various conditions, such as between floors and inside of offices [5] [6]. Studies have also been performed for various outdoor or between-building environments [2][4]. However, far fewer studies have been performed on small-scale fading.

The purpose of this study is to measure and characterize small-scale fading for a realistic, indoor propagation environment.

Experimental/Computational Method

For this experiment, a custom quarter-wavelength monopole antenna was used in combination with an amplifier and a bandpass filter to form a receiver, while a spectrum analyzer in conjunction with a computer system recorded data. A pure tone signal was generated using two signal generators and a frequency mixer, amplified, and transmitted at a frequency of 2.43 GHz from an omnidirectional antenna located more than ten wavelengths from the receiver. The receiver was mounted on a linear positioner, and measurements were taken at regular intervals as it was moved down the track. Figure 1 shows the different parts of a typical setup.



Figure 1a: Receiver apparatus, mounted to a linear positioner.



Figure 1b: Transmitter apparatus, as mounted for the line-of-sight measurements.

Measurements were conducted in a lab room on the top floor of the Van Leer building at the Georgia Institute of Technology. The room is approximately 3 ½ meters wide and 7 meters long, and contains a large number of scatterers, distributed around the sides of the room. Of particular note are two large metal cabinets which were on the far side of the room from the transmitter, facing back towards the transmitter.

As a check on the instruments and processing, data was taken on the noise present in the channel when no transmitted signal was present. For the next set of measurements, the transmitter was placed just outside of the room with a clear line-of-sight (LOS) through an open doorway for

the entire area over which the measurements were made. Subsequently, data was also taken with the transmitter placed behind the wall adjoining the doorway, and with the transmitter placed over 7 meters down the hallway with several walls and two offices between the transmitter and receiver on the direct LOS path.

Subsequent analysis was performed using MATLAB and commonly known distribution types. Standard parameter finding methods were used to find the variance and mean for a Rayleigh fit to the data. In order to obtain an unbiased Ricean fit, a Maximum Likelihood (ML) estimator put forth by Sijbers et al. was used [7]. Taking a cue from the Ricean fitting method, a ML estimator was devised for use in fitting a Two-Wave-Diffuse-Power (TWDP) curve.

Results and Discussion

Data was first taken on the noise in the system: the receiver apparatus was connected, but without any transmitted signal, and data was collected at the same frequency as it would be later in the experiment. This was done in order to ascertain the noise level in the system. In subsequent measurements, any measurement indistinguishable from noise could be discarded based on this data, though in practice the signal turned out always to be strong enough that this was not necessary. Figure 2 shows the histogram of this data with an overlaid Gaussian fit. As expected, this data was Gaussian distributed. The variance in the noise in the system was found to be about 0.841 μW (-30.8 dBm). There was some 802.11 interference, seen as an outlier point in the graph. The occurrence of this event was felt to be sufficiently low (1 out of more than 2000 uncorrelated measurements) as to not interfere with further measurements.

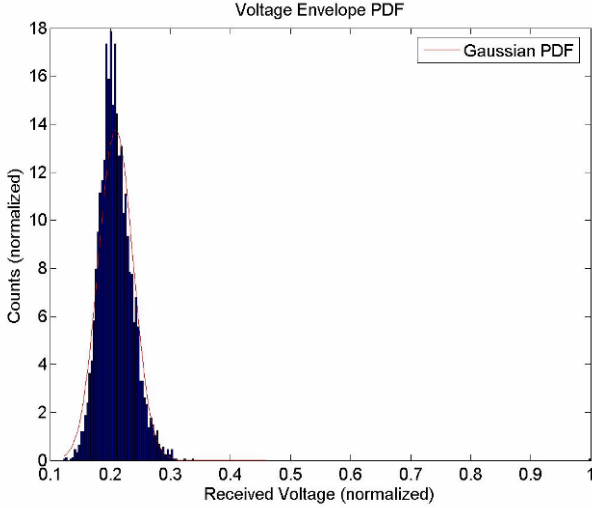


Figure 2: Histogram for noise data. Received voltage magnitude is normalized so that the highest value is 1.

The data was first normalized such that the highest value was set equal to zero dB, then converted to a linear scale from the original logarithmic form, thus making the subsequently constructed graphs more readable. Subsequently, histograms were constructed from the data, and probability density functions (pdfs) generated in the aforementioned manner. In order to obtain a TWDP fit, numerical techniques were found to be impractical. Consequently, the approximation:

$$F_R(r) = \frac{r}{\sigma^2} \exp\left(\frac{-r^2}{2\sigma^2}\right) * \sum_{i=1}^M a_i D\left(\frac{r}{\sigma^2}; K, \Delta \cos \frac{\pi(i-1)}{2M-1}\right), \text{ where } r \text{ and } \sigma^2 \text{ are as defined previously,}$$

$K = \frac{V_1^2 + V_2^2}{2\sigma^2}$, where V_1 and V_2 are the magnitudes of the voltages of the specular components,

$$\Delta = \frac{2V_1V_2}{V_1^2 + V_2^2}, \text{ and}$$

$$D(x; K, \alpha) = \frac{1}{2} \exp(\alpha K) I_0(x\sqrt{2K(1-\alpha)}) + \frac{1}{2} \exp(-\alpha K) I_0(x\sqrt{2K(1+\alpha)})$$

, where $I_0(\cdot)$ is a zeroth-order modified Bessel function of the first kind, and the a_i are coefficients, formulated by Durgin et al. in [8] was used, to fifth order in i . It is worth noting that using ML theory, the log-likelihood function for this formula results in more than one local maximum in V_1 , V_2 , and σ in the range for all three parameters ≥ 0 , requiring one to compare the values at all such points to find the global maximum. In testing this method on the data gathered, at least 2 local maxima in that range always resulted: one with V_1 and V_2 nearly equal, one with V_2 nearly equal to zero. In some tests, a third point appeared, wherein the value for K would be exceptionally small (low signal-to-noise ratio (SNR)). This third point was not considered in later tests, owing to the SNR being obviously higher than that given by this point.

Figure 3 shows histograms from a few representative data runs, with various probability density functions overlaid. For the data set in 3a, the K -value for the Ricean distribution was found to be 4.7 dB, using the ML estimator mentioned above. While a Ricean distribution was expected since there was a strong line-of-sight component, the fit for this distribution was bad, with a root-mean-squared (rms) error of 0.49 normalized counts, which was still significantly better than the Rayleigh fit, which had an rms error of 0.59 normalized counts, some 20% higher. For comparison, the rms error of the Ricean fit in figure 3b, which is visually Ricean distributed, is 0.38 normalized counts, a good 22% lower. In all, for the four runs where there was an unobstructed line-of-sight between the transmitter and the receiver, two showed the expected Ricean distribution as in figure 3b,

one showed a Rayleigh distribution, as in figure 3c, and that shown in figure 3a did not adequately fit any of the standard pdfs. For the trial which showed a Rayleigh distribution, it was hypothesized that part of the transmitter's line-of-sight may have been blocked by the door, and the transmitter was subsequently moved slightly to reduce this possibility, though such obstruction was not clearly ascertainable. For the two measurements taken with a wall between the transmitter and receiver along the line-of-sight, one trial showed a Ricean distribution, leading to suspicion that the wall was letting a significant amount of signal through, and one showed a distribution comparable to that in 3a. While detailed tests on this were not conducted, there appeared to be a loss of from 4 to 11 dB through the wall at this frequency: not enough to eliminate the LOS component for this equipment, merely lowering the measured voltage levels. See table 1 at the end of this section for the values of the rms error for all three fits for all eight trials.

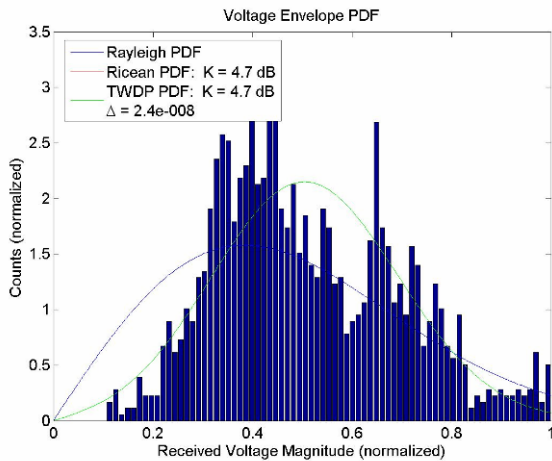


Figure 3a: Histogram of received voltage magnitude measured in a local area with overlaid pdf models. The received envelope is normalized such that the highest value is set to 1. Note that the Ricean and TWDP PDFs are not visually distinguishable.

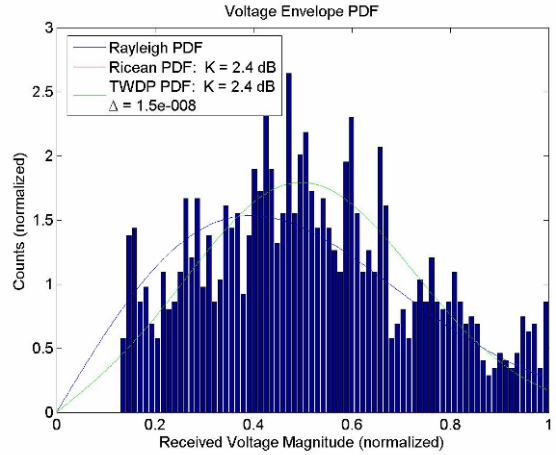


Figure 3b: Histogram of received voltage magnitude measured in a local area with overlaid pdf models. The received envelope is normalized such that the highest value is set to 1. Note that the Ricean and TWDP PDFs are not visually distinguishable.

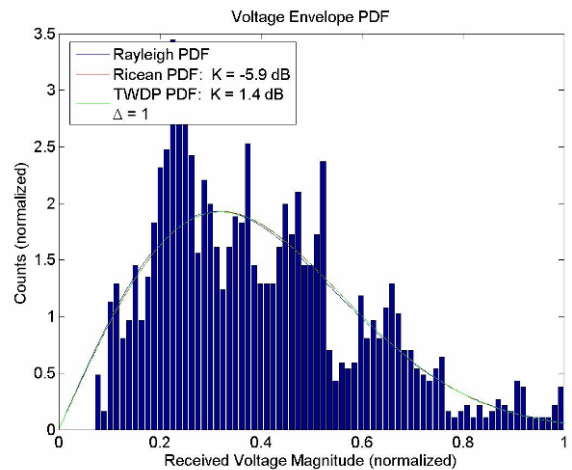


Figure 3c: Histogram of received voltage magnitude measured in a local area with overlaid pdf models. The received envelope is normalized such that the highest value is set to 1. Note that the three PDFs are not visually distinguishable.

Figure 4 shows plots of received voltage (with the same normalization applied as in figure one) versus position for the same data runs as in figure 1. As expected, the distribution is effectively random, without any noticeable decrease in received signal strength as a result of increased distance from the transmitter, except in the case of 4b, where there is a slight decrease between

the beginning and the end in terms of peak height. This corresponds to the Ricean-distributed sets, but this was not a consistent trend among the other such sets, which showed the expected random variance.

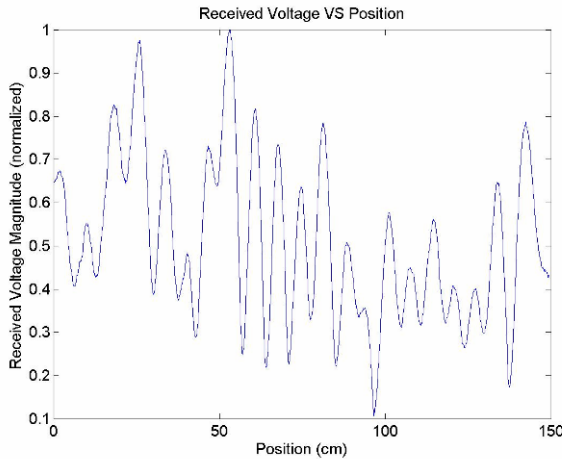


Figure 4a: Graph of a small-scale fading received envelope versus position in centimeters, corresponding to 2a. Received voltage is normalized such that the highest value is 1.

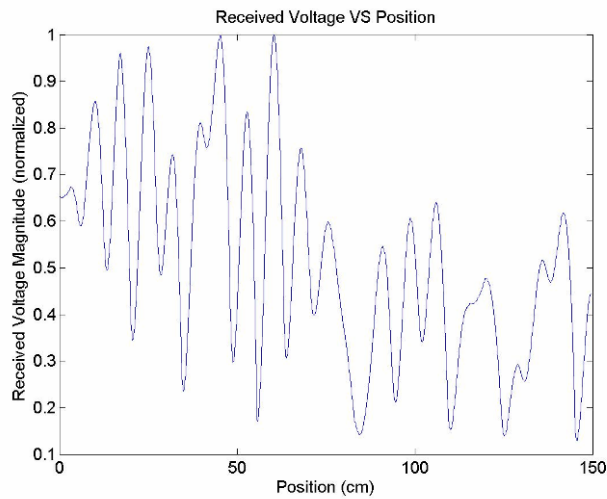


Figure 4b: Graph of a small-scale fading received envelope versus position in centimeters, corresponding to 2b. Received voltage is normalized such that the highest value is 1.

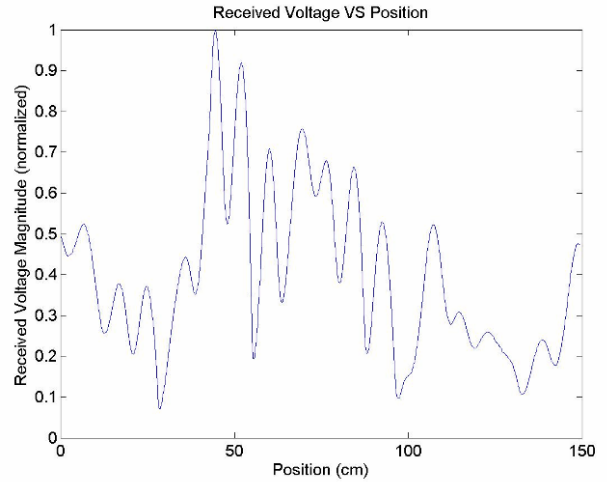


Figure 4c: Graph of a small-scale fading received envelope versus position in centimeters, corresponding to 2c. Received voltage is normalized such that the highest value is 1.

For the measurements taken with the transmitter located down a hallway with any line-of-sight component reduced to a non-specular component, neither of the two data runs showed a Rayleigh distribution, as was expected, and in fact, neither fit any of the tested pdfs very well, with the closest in each case being a Rayleigh distribution, with rms error of 0.51 in one case and 0.64 in the other, with the TWDP and Ricean pdfs being clearly distinguishable from the Rayleigh pdf in both cases. The histograms and overlaid pdfs for these graphs are seen in figure 5. It should be noted that due to the fact that the hallway in question was in use at the time of measurements, the channel was necessarily time-varying during the taking of this last group of measurements.

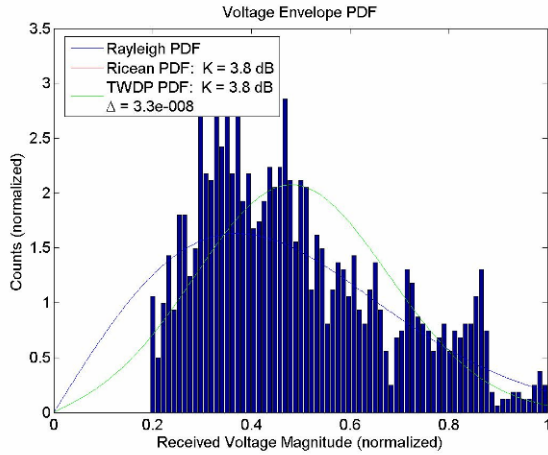


Figure 5a: Histogram of received voltage magnitude measured in a local area with overlaid pdf models. The received envelope is normalized such that the highest value is set to 1. Note that the Ricean and TWDP pdfs are not visually distinguishable.

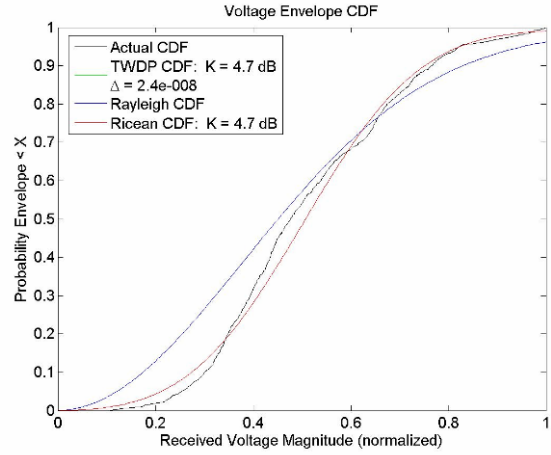


Figure 6a: Cdf for the data with cdfs of other fits overlaid, corresponding to the pdfs of figure 3a. The received envelope is normalized such that the highest value is set to 1. Note that the Ricean and TWDP pdfs are not visually distinguishable.

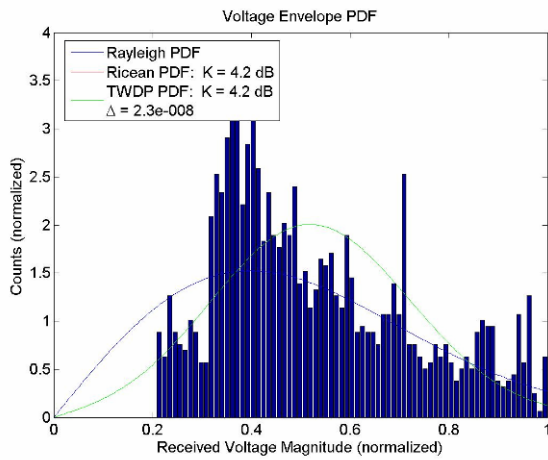


Figure 5b: Histogram of received voltage magnitude measured in a local area with overlaid pdf models. The received envelope is normalized such that the highest value is set to 1. Note that the Ricean and TWDP pdfs are not visually distinguishable.

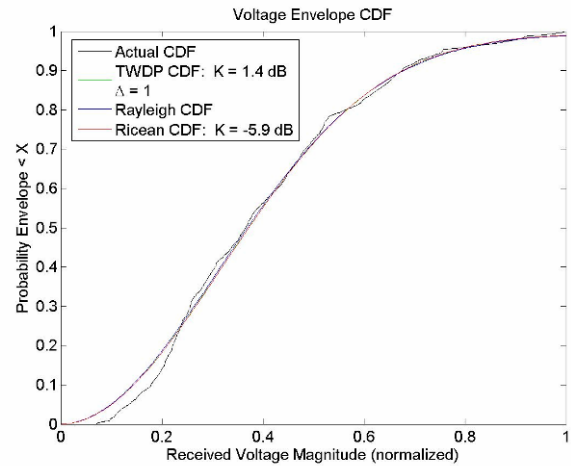


Figure 6b: Cdf for the data with cdfs of other fits overlaid, corresponding to the pdfs of figure 3c. The received envelope is normalized such that the highest value is set to 1. Note that the Ricean and TWDP pdfs are not visually distinguishable.

Cumulative distribution functions (cdfs) were also constructed using a Riemann summation, and in these how well a particular pdf fits is often clearer. A few of these are given in figure 6, corresponding to 3a, 3c, and 5b.

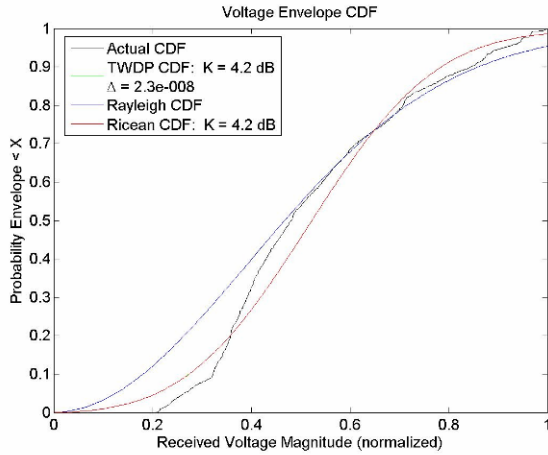


Figure 6c: Cdf for the data with cdfs of other fits overlaid, corresponding to the pdfs of figure 5b. The received envelope is normalized such that the highest value is set to 1. Note that the Ricean and TWDP cdfs are not visually distinguishable.

For all data runs, the TWDP fit was visually indistinguishable from the Ricean fit: Indeed, the value for Δ was always negligibly close to either zero or one: one in the case where the graph was most nearly Rayleigh distributed and zero otherwise. In addition, when the value for Δ was close to 0, the precise value obtained was sensitive to changes in the initial test points used for parameter estimation, though within the same order of magnitude. Furthermore, while many of the data sets failed to fit any of the traditionally used PDFs, in all cases less time was spent in the region of low signal strength than in the Rayleigh case.

Trial #	Type	Rayleigh rms error	Ricean rms error	TWDP rms error
1	LOS	0.592	0.488	0.488
2	Through wall	0.461	0.355	0.355
3	Through wall	0.568	0.538	0.538
4	LOS	0.401	0.378	0.378

5	LOS	0.433	0.437	0.436
6	LOS	0.551	0.500	0.500
7	Down hall	0.506	0.554	0.554
8	Down hall	0.644	0.670	0.670

Table 1: Table showing the rms error for the fits of various pdfs for the different measurement trials. Note that rms error has units of normalized counts.

Conclusions

Rayleigh or Ricean distributions may not always be adequate in describing small-scale fading for indoor propagation environments. When designing an indoor network, particularly if the transmitter and receiver(s) are located in an open area, one should be wary of this possibility. Particularly, it is highly recommended that any fading model which has fewer undesirable drops in signal strength than a Rayleigh model be used with extreme caution, particularly in the most common circumstances where the channel is time-varying, since it is a distinct possibility that the actual distribution will not fit these models particularly well, but the data shows that it is very unlikely that the actual distribution will have *more* such drops than it would under a Rayleigh model.

Furthermore, while TWDP fading may describe the most fading scenarios mathematically, in that it reduces to all other common distributions in different limiting cases [8], these tests show that an indoor fading environment can be described just as accurately by a Ricean distribution in most cases.

Also, the transparency of interior building walls may be high enough at around 2.4

GHz to allow a significant signal to pass through a single wall, which can be factored into making a wireless network serviceable with fewer terminals in an area with enclosed rooms. However, it should be noted that the results obtained in this respect were rather preliminary, and so further investigation is required.

Furthermore, the use of a linear positioner has, in this basic experiment, been shown to provide a means of mapping small-scale fading phenomena in the wireless channel to a fairly high level of precision in the GHz range. Further investigation in this direction may result in more detailed characterization of small-scale scattering and fading phenomena.

References

[1] G. D. Durgin, *Space-Time Wireless Channels*. Upper Saddle River, NJ: Prentice Hall, 2003.

[2] A. Fanimokun and J. Folik, "Effects of Natural Propagation Environments on the Wireless Sensor Network Coverage Area," *Proceedings of the 35th Southeastern Symposium on System Theory, 2003*, 16-18 March 2003.

[3] J. Frolik, "A Case For Hyper-Rayleigh Fading Channels," *IEEE Transactions on Wireless Communications*, Vol. 6, no. 4, pp. 1235-1239, April 2007.

[4] K. P. McCarthy and U. Wellens, "Measurements of 900 MHz Propagation for Microcellular Communications Systems Design," *8th European Conference on Electrotechnics, 1988. Conference Proceedings on Area Communication, EUROCON 88*, Stockholm, Sweden, 13-17 June 1988.

[5] R. R. Murray, H. W. Arnold, and D. C. Cox, "815 MHz Radio Attenuation Measured Within A Commercial Building," *IEEE Transactions on Antennas and Propagation*, vol. 37, issue 10, pp. 1335-1339, Oct. 1989.

[6] P. Nobles and F. Halsall, "Indoor Propagation at 17GHz and 60GHz – Measurements and Modeling," *IEE National Conference on Antennas and Propagation, 1999*, York, UK, 31 March-1 April 1999.

[7] J. Sijbers, A. J. Den Dekker, D. Van Dyck, and E. Raman, "Estimation of Signal and Noise from Rician Distributed Data," *Proceedings of the International Conference on Signal Processing and Communications*, pp. 140-142, Gran Canaria, Canary Islands, Spain, 11-14 February 1998.

[8] Gregory D. Durgin, Theodore S. Rappaport, and David A. de Wolf, "New Analytical Models and Probability Density Functions for Fading in Wireless Communication," *IEEE Transactions on Communications*, Vol. 50, No. 6, pp. 1005-1015, June 2002.

Acknowledgments

This work was supported by the STC Program of the National Science Foundation No. DMR 0120967, and CHE 0453596.



Alexander H. Henderson was born in Aiken, South Carolina on June 19, 1986. A current undergraduate at Furman

University, Greenville, SC, he anticipates graduating in 2008 with a B. S. in Physics and Mathematics. After graduation, he intends to pursue a Ph.D. in Physics.

A member of the Society of Physics Students and Sigma Pi Sigma (a physics honors society), Mr. Henderson has previously done undergraduate research in the field of gravitation under Dr. William Baker at Furman University.